7th International Conference on Multiphase Flow,
ICMF 2010, Tampa, FL, May 30 – June 4, 2010

Aeration in lubrication flows with application to reduced disengaged drag torque in clutches

C.R. Aphale*, W.W. Schultz† and S.L. Ceccio†

* Department of Mechanical Engineering, University of Michigan, Ann Arbor, MI 48109, USA

Presently with ExxonMobil Upstream Research Company, Houston, TX 77098, USA

† Department of Mechanical Engineering, University of Michigan, Ann Arbor, MI 48109, USA

caphale@umich.edu, schultz@umich.edu and ceccio@umich.edu

Keywords: aeration, clutches, disengaged drag, lubrication

Abstract

The aeration of an oil film flowing between the faces of two closely spaced circular plates (one stationary, and one rotating) is examined experimentally, numerically, and with an improved lubrication model. The gap between the plates is small compared to their radii, making lubrication theory appropriate for modeling the flow. However, standard lubrication boundary conditions suggested by Reynolds (1886) of $p = 0$ and $p_n = 0$ (Dirichlet and Neumann conditions on pressure) at the gas-liquid interface do not allow for the inclusion of a contact line model, a phenomenon that is important in the inception of aeration. Hence, the standard theory does not adequately predict the experimentally observed onset of aeration. In the present work, we modify the Neumann boundary condition to include both interfacial tension effects and the dynamics of the interface contact angle. The resulting one-dimensional Cartesian two-phase model is formulated to incorporate the prescribed contact line condition and tracks the interface shape and its motion. This model is then implemented in an axisymmetric, two-dimensional model of the rotating disk flow and used to predict the onset of aeration for varying surface tension and static contact angles. The results of the modified lubrication model are compared with experimental observations and with a numerical computation of the aerating flow using a Volume of Fluid method.

1 Introduction

In a disengaged or open clutch, one plate typically rotates while the other is stationary. Oil is passed between open clutch plates to provide lubrication during clutch re-engagement and to transfer heat away from the plates. But the shearing of this liquid between the open clutch plates results in viscous drag. Consequently, it is beneficial to introduce air between the two plates while they are disengaged, reducing the drag and subsequent parasitic losses. Open-clutch drag has been examined by Schade (1971), Lloyd (1974), Fish (1991), Aphale *et al.* (2006) and Aphale *et al.* (2010). Schade first suggested that air might be present between the plate surfaces at high rotation rates, which was subsequently observed to occur. Aphale *et al.* (2006) examined the conditions necessary for incipient aeration, and Aphale *et al.* (2010) studied how the presence of grooves on the face of one plate can enhance the aeration process. In the present work, we examine how lubrication theory, appropriately formulated, can be used to predict the onset of aeration between two rotating disk, the geometry of a typical set of clutch plates. We will show how the interfacial properties of the fluid and gas (e.g. the oil and air) strongly influence the conditions for the inception of aeration in lubricating flow.

Figure 1 presents a schematic diagram of the flow geometry under consideration. Two disks, separated by a narrow gap, are rotating about the same axis. A pocket is present in one disk, producing an annular ring of inner radius R_i and outer radius R_o. The minimum spacing between the plates is h. The radial and axial dimensions are r and z, as shown. A liquid is pumped into the cavity between the disks at an inlet that lies along the axis of rotation, and the liquid flows both circumferentially and radially until it exits from the gap at the outer radii of the disks. Important parameters include the flow rate of the liquid, Q, and the properties of the fluid (usually an oil) such as the density, ρ, viscosity, μ, and surface tension, σ. The drag torque that is developed between the plates is T, and in the present study, we will consider one plate rotating with speed ω, and one stationary plate. Note

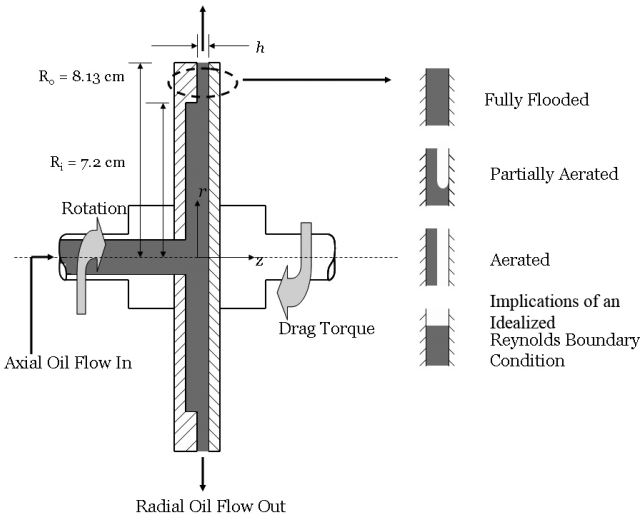

Figure 1: Schematic of the experimental assembly (left) with different modes of aeration shown (right). Liquid flows in axially from a passage within the rotating shaft and is expelled radially outward due to the centrifugal action of the rotating plate. When aeration occurs, the gas interface moves radially inwards, with the gas layer forming on the stastionary plate.

that a finite flow of fluid through the gap can occur simply as a result of centrifuging, but in the present case, the flow rate of liquid will be prescribed via pumping.

Aeration can occur naturally between the rotating disks due to centrifugal forces that act on the liquid flowing through the gap. Figure 1 also shows the type of aerated flows that could develop in the gap between the plates. Without aeration, the flow is considered fully flooded. But, under certain flow conditions, a pocket of gas can penetrate from the outer radii of the disks to partially aerate the gap flow. The cavity usually forms on the stationary plate. If the gas pocket extends across the radial extent of the gap, the flow is fully aerated. Also shown is an idealized topology of the air pocket that will be discussed below. The onset of aeration on smooth clutch plates (e.g. without surface grooves, roughness, or other patterns) depends on a variety of flow and physical parameters, including the rotation rates of the plates, the liquid flow-rate, the liquid properties and the gap thickness. Air penetration toward the inner radii of the clutch plates necessitates the formation of a free surface and contact line on the drying, stationary plate. This suggests that interfacial properties of the oil and plate surfaces will be an important consideration.

The gap between the two plates is small compared to the plate radii. Therefore, lubrication theory can be successfully used to model the flow (Aphale *et al.* (2006)). However, difficulties with the standard lubrication model are encountered during the onset and development of aeration since aeration in lubricating flows depends strongly on the contact line condition. Reynolds (1886) proposed a simple gas-liquid interface conditions for lubricating flow where $p = 0$ and $p_n = 0$ (Dirichlet and Neumann conditions on pressure) at the gas-liquid interface. The former interface condition is justified since the pressure in the gas is negligible compared to that of the liquid. And when the cavity is open to the environment (as in the case studied here), the gauge pressure is considered zero.

In cavitating lubrication flows, the fluid continues to flow beyond the interface, but only along one wall. We will model this flow in a way that incorporates surface tension and contact line physics. The aeration process under consideration here is analogous to other interfacial flows, such as the progression of long bubbles in tubes modeled by Bretherton (1961). The flow was divided into three regions: 1) the leading spherical cap, 2) the intermediate region where the shape of the bubble is set by surface tension, and 3) the final asymptotic region where the bubble and tube form an annulus and the thickness of fluid in the tube remains unchanged. Bretherton's analysis can be modified for flow between two flat plates, and it provides a steady solution for the shape of the interface and accurately predicts the pressure in the intermediate region. However, the solution employs two assumptions that make it unsuitable for predicting aeration in the present problem. First, the interface shape is assumed to be steady in the frame moving with the bubble. Second, a zero wall contact-angle is imposed on the flow. Both these assumptions need to be relaxed for modeling the aerating flow between the plates.

Dussan (1979) discussed the relationship between the contact angle and speed of a moving contact line. Since, the stress singularity at the contact line makes the mathematical problem ill posed, researchers have developed empirical contact line models relating the two quantities that introduce contact line slip. The most commonly used model has a hysteresis region where the velocity is zero between an advancing and receding contact angle. In the present work, we will employ a contact line model based on the theory of Hocking (1976) that has no hysteresis region, as discussed below. We will combine this contact line model with lubrication theory to predict the unsteady aeration between the clutch plates. Finally, the results of this model will be compared to experimental observations of a canonical aerating flow and the results of a Volume Of Fluid (VOF) numerical model formulated with commercial code FLUENT®.

2 Experimental observation of aeration

An experimental apparatus was constructed to examine and measure the aerating flow between a rotating and stationary disk as shown in Figure 1. Aphale *et al.* (2006) provide a detailed description of the setup, instrumentation, and procedure. The apparatus had R_i = 7.20 cm, and outer radius R_o = 8.13 cm, making $R_m = (R_i + R_o)/2$ = 7.7 cm and $\delta R = (R_o - R_i)$ = 0.93 cm. The rotation rate of the moving disk was $0 < \omega <$ 3500 RPM. The minimum gap between the plate, h, was varied between $100 \pm 20 < h < 200 \pm 20$ microns, and plates were parallel to within ± 10 microns. The torque on the stationary disk was measured with a moment arm and linear force transducer for $0 < T < 1.5$ N m. A syringe pump was used to meter the liquid flow between the plates at a rate of Q = 100 $\pm$ 5 mL/s. The stationary plate was made from aluminum or aluminum coated with a 100-micron thick layer of Polytetrafluoroethylene (PTFE) (commonly known as Teflon). The rotating plate was made from quartz for optical access.

The fluid used in the experiments was standard automatic transmission fluid that was maintained at a nominal temperature of 20 to 25 C. The fluid density was ρ = 873 kg / m^3, and the viscosity was μ = 0.048 N s /m^2. The surface tension of the fluid was measured with a Langmuir type device (Lapham et al., 1999) to be 0.029 $\pm$ 0.001 N/m at the operating temperature. The static contact angle was measured on the aluminum and Teflon coated disks using a sessile drop experiment. The measured static contact angle for oil on aluminum was $\theta_C = 9^o \pm 1^o$ and $\theta_C = 45^o \pm 1^o$ for the oil on Teflon.

Figure 2 presents typical data for the drag torque, T, as a function of rotation rate, ω. The data are shown for the aluminum disk and two runs of the Teflon coated disk. Note that the drag torque increases with increasing rotational speed until there is a sharp drop, corresponding to the onset of aeration. The torque ranges from 0.2 $< T <$ 0.8 N m over a range of $500 < \omega <$ 3500 RPM with the oil flow rate fixed at Q = 100 mL / s. These data represent Reynolds numbers $Re = \rho\omega R_m h/\mu$ in the range $7 < Re <$ 52, and Weber numbers $We = \rho\omega^2 R_m^2 h/\sigma$ in the range $49 < We <$ 2400. The non-dimensional flow rate $Q = Q\mu/\rho\omega^2 R_m^2 h^3$ is in the range $7 < Q <$ 338, and the non-dimensional Torque, $T = Th/\mu\omega R_m^4$, is in the range $0.13 < T < 0.2$.

3 Two-dimensional axisymmetric multi-phase numerical modeling using the Volume of Fluid method

A two-dimensional axisymmetric geometry conforming to the above experimental geometry was implemented for use in a Volume of Fluid (VOF) formulated in FLUENT® simulation of the aerating flow. GAMBIT® was used to create the grid, which had 200 x 75 node points in the radial and axial directions, respectively. The grid in the axial direction was refined near the walls to resolve the steep flow gradients expected there. At the inlet, natural boundary conditions are prescribed while at the outlet ambient pressure boundary conditions are used. The fluid flow passing from the inlet at the axis, through the region with the larger gap was first simulated and used as an inlet condition for the flow leading into the narrow gap at the outer radii. The computations are first order accurate in time and space. The time step used is 0.001 seconds.

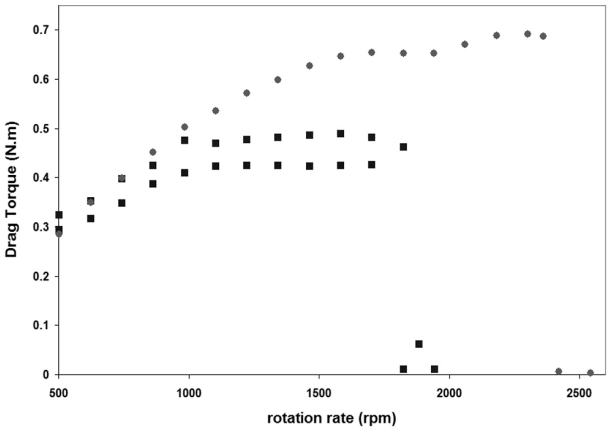

Figure 2: The experimentally obtained results of coating the Aluminum disk with Teflon. The two curves for Teflon coated stationary plates are shown with squares. The circles denote the case when the stationary plate surface is aluminum.

Figure 3 presents a plot of the computed drag torque versus rotational speed for the conditions matching that of the experiment. As the speed of rotation increases, the transmitted drag torque increases nearly linearly, as expected. However, at a critical rotational speed, the torque falls abruptly to near zero levels as a result of aeration. The rotation speed at which aeration occurs is sensitive to the surface tension, as shown in Figure 3, and to the imposed contact angle, as shown in Figure 4.

The trend in figure 3 shows that increasing the value of surface tension promotes aeration. This trend can be explained on the basis of pressure-curvature relation. Ignoring viscous normal forces,

$$\delta p = \sigma(\frac{1}{R_1} + \frac{1}{R_2}) \tag{1}$$

where δp is the pressure increase on the concave side of the interface, and R_1, R_2 are the principal radii of

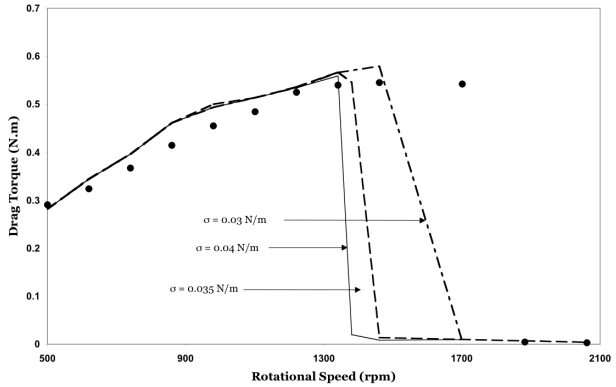

Figure 3: The drag torque, T, versus the rotation rate, ω, as computed with the Volume of Fluid model. The sharp drop in drag torque at a particular rotation rate is coincident with aeration. An increase in the surface tension promotes aeration. The computations were performed using the contact angle of the aluminum plate, and the corresponding experimental results are shown (circle)

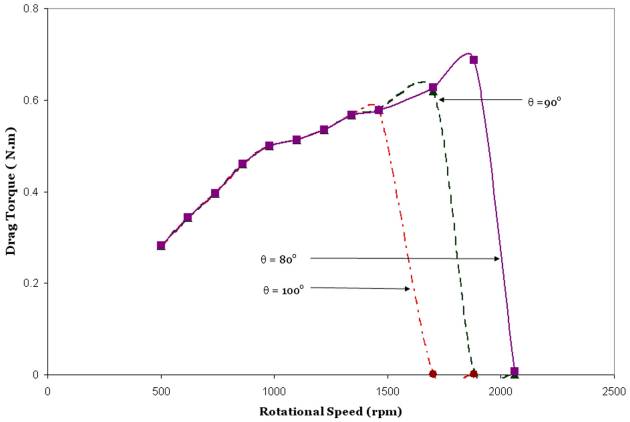

Figure 4: The drag torque, T, versus the rotation rate, ω, as computed with the Volume of Fluid model, illustrating the influence of the contact angle on the inception of aeration. A larger contact angle, θ_c, indicates a lesser affinity for the liquid, and, as a result, aeration is promoted as the contact angle increases.

curvature of the interface. The shape of the aerating interface is such that the concave side is exposed to gas, and the higher pressure on the concave side of the interface pushes the air toward the inner radius. Therefore, for a given interface shape, increasing the magnitude of the surface tension will promote aeration.

When the clutch aerates, a gas layer forms on the stationary plate since the centrifugal acceleration of liquid near the stationary plate side is low compared to that near the rotating plate. This leads to the formation of a potentially unsteady contact line, where the liquid-gas interface intersects with the stationary plate, and in the two-dimensional case this line moves radially inwards or outwards, depending on whether the clutch is aerating or flooding. The results in Figure 4 were obtained by varying the static contact angle while keeping the surface tension fixed. A higher contact angle signifies an oleophobic behavior of the stationary plate for the case of an oil flow, which would promote the formation of an air layer. However, the strong inertial action near the rotating plate ensures that the oil continuously forms a thin film on its surface. Thus, altering the contact angle of the rotating plate will have a reduced effect on aeration.

The contact angle was modified experimentally by coating the stationary plate with an oleophobic substance (Teflon). The experimental data presented in Figure 2 illustrates the effect of contact angle on the inception of aeration. The two data sets for the Teflon coated plate are two separate experimental runs to illustrate the experimental repeatability. We can see some difference in the drag torque when it is still flooded. However, the aeration incipience is earlier than the plate without Teflon. The experiments are performed at a fixed clearance and oil flow rate, and the drive motor spins the rotating disk at a low rotational speed to start and the speed is increased until aeration is observed. These observations are consistent with the numerically predicted influence of the contact angle variation on aeration.

4 Modification of the two-phase lubrication model in two-dimensional flow

Both the experiments and the VOF computations demonstrate that both the surface tension and flow physics at the contact line significantly affects the incipience of aeration. If lubrication theory is to be employed to predict the onset of aeration between the disks, these physical processes, must be incorporated into the lubrication model. In this section, we will formulate the required modifications for an aerating flow in two-dimensions.

If the static contact angle determines the hydrostatic displacement of a liquid column in a capillary, the dynamic contact angle determines the rate of the displacement. The non-integrable stress singularity at the contact line when no slip is applied makes the mathematical problem ill-posed. Consequently, a simple analytic model between the dynamic contact angle and contact line speed is difficult to formulate. Various authors have developed empirical contact line models, and Dussan

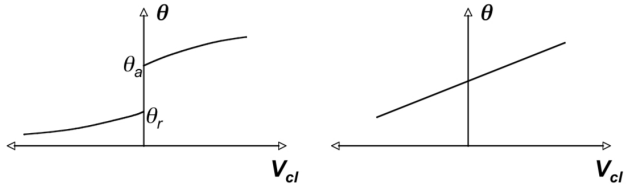

Figure 5: Commonly used contact line models relating the contact angle, θ_c, with the velocity of contact line, V_{cl}. The common model is shown on the left, the model proposed by Hocking (1976) is shown on the right.

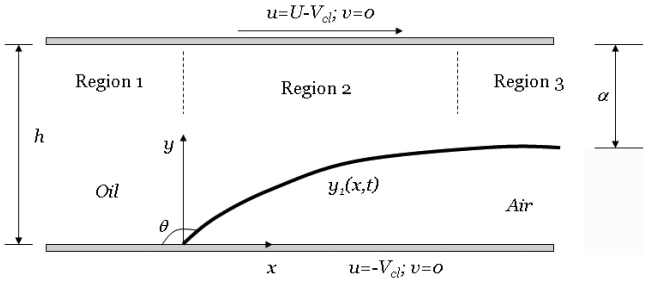

Figure 6: The geometry of the two-dimensional model using Cartesian coordinates. The coordinate system moves with the velocity of the contact line, V_{cl}. The fluid attaches to the moving plate while the gas attaches to the stationary plate.

(1979) provides a summary. The most common model is illustrated in Figure 5 (on the left) and has a hysteresis region bounded by an advancing and receding contact angle. The simpler model (on the right) proposed by Hocking (1976) has no hysteresis region and has a single static contact angle, which is appropriate for smooth surfaces. Here we will employ a model similar to that of Hocking that has a hyperbolic tangent profile. Note that the velocity of the contact line may be positive or negative for the same contact angle.

Bretherton (1961) analyzed the motion of elongated bubbles in tubes and observed that the actual velocity of the bubbles was larger than that of the fluid, since the bubbles 'did not behave like close-fitting pistons'. In the absence of flow, the surface tension alone governs the shape of the bubble and the bubbled ends become hemispherical caps. For sufficiently small values of $\mu U/s$, Bretherton divided the bubble interface into three regions: 1) the fully flooded region, 2) the intermediate region where the shape asymptotes to a final film thickness, and 3) the final region where the film thickness is constant and there is no pressure driven flow. He assumed that surface tension alone governs the interface shape and that viscous stresses are negligible away from the wall. Thus, in this region $p_x = -\sigma y_{1xxx}$, where y_1 is the location of the interface and is only a function of x and t, where the subscripts x and y denote differentiation with respect to the spatial coordinates. Bretherton's analysis was for a wall contact angle of zero. Our goal here is to incorporate the moving contact line model of Hocking described above with his analysis.

A modified Bretherton model is obtained by analyzing the problem in the contact line frame of reference where the contact line moves with the velocity V_{cl}. The contact line often accelerates or decelerates and hence the analysis should be performed in an inertial frame of reference. However we assume that the forces due to accelerations are small compared to other forces acting on the interface. A schematic of the model geometry is shown in Figure 6. In the contact line frame of reference, the velocity of the top plate is $U - V_{cl}$, and that of the bottom plate is $-V_{cl}$. It is best to analyze the flow in three separate regions. Region 1 is the fully flooded region (x < 0) where the momentum equation reduces to the standard lubrication form

$$u_{yy} = p_x/\mu \tag{2}$$

$$p_y = 0. \tag{3}$$

(2) can be integrated using the no slip boundary conditions. The pressure gradient p_x in this region is just a constant and obtained from the flow rate Q'. The flow region where the film thickness remains constant (α) is Region 3. In this region the flow is purely wall driven and p and p_x are both zero. The velocity profile is rectilinear and the film thickness is calculated by a simple mass balance in the contact line frame of reference,

$$Q' - V_{cl}h = (U - V_{cl})\alpha. \tag{4}$$

The flow region from the contact line until where the interface flattens out is Region 2. According to Bretherton, surface tension alone determines the interface shape at sufficiently low $\mu U/\sigma$. We still assume (2) and (3) to hold true; a good assumption to make if the contact angles are low. Thus from (2) we again obtain the x component of velocity and the flow rate. If the interface shape does not change with time, then the flow rate balance between Regions 2 and 3 leads to the following condition on pressure

$$p_x = -3\mu U \frac{(h-\alpha) - y_1}{(y_1 - h)^3}. \tag{5}$$

Here p_x and y_1 are functions of x.

Combing this with $p_x = -\sigma y_{1xxx}$, the governing differential equation for the steady shape of the interface

is,

$$y_{1xxx} = 3\mu U/\sigma \frac{(h-\alpha)-y_1}{(y_1-h)^3}. \quad (6)$$

The correct boundary conditions to be prescribed are $y_1(0,t) = 0, y_{1x}(\infty,t) = 0, y_{1x}(0,t) = \tan(\pi-\theta)$. (5) is a nonlinear ordinary differential equation that can be solved using a two-point shooting method. This modified Bretherton's model for a flow attached to a flat plate now incorporates the contact line model and predicts the steady shape of a moving interface.

However, Bretherton's model can be used to obtain a $posteriori$ the shape of the interface if V_{cl} is provided but cannot predict when aeration will occur. Moreover, Bretherton's model is steady and aeration may only occur for unsteady flows. The contact line condition determines V_{cl}/U and then (4) requires unphysical values of Q/Uh and α/h, which must lie between 0 and 1 for steady flows. An unsteady Bretherton model must then be used. The interface shape is advanced by a time stepping procedure as described below. The normal stress boundary condition is simplified to neglect the viscous stresses terms. The pressure as $x \to \infty$ is taken to be zero (atmospheric) and air is assumed to be passive. Thus, the expression for pressure on the fluid side of the interface is

$$p(x,t) = -y_{1xx} \quad (7)$$

assuming a low slope consistent with the lubrication theory. Using $p(\infty,t) = 0$, $p_x(x,t)$ and $p_{xx}(x,t)$ can be computed. Here, $y_{1x}(0,t)$ is the tangent of the contact angle determined from the contact line model, here modeled by this simple expression

$$V_{cl} = \frac{1}{1000}\tanh^{-1}(\theta-\theta_{st})(\theta_{max}-\theta_{st})^{-1}, \quad (8)$$

where θ_{st} is the static contact angle and θ_{max} is the maximum contact angle in the appropriate quadrant. Then, the x-component of velocity is integrated from the momentum equation. The zero tangential stress boundary condition on the interface and no slip condition on the top wall yield

$$u(x,y,t) = \frac{p_x}{\mu}\Big(\frac{y^2-h^2}{2} + y_1(h-y)\Big) + U - V_{cl}. \quad (9)$$

Note that in this region, u is a function of all three variables x, y, t, since p_x and y_1 are x-dependent. We calculate v from continuity,

$$u_x + v_y = 0. \quad (10)$$

A straightforward integration of u_x leads to the expression for v on the interface as

$$v(x,y,t) = \frac{p_{xx}}{\mu}\frac{(y_1-h)^3}{3} + \frac{p_x}{\mu}y_{1x}\frac{(y_1-h)^2}{2}. \quad (11)$$

Finally, the kinematic boundary condition is satisfied to march in time and to solve for y_1

$$y_{1t} + u(x,y,t)y_{1x} = v(x,y,t), \quad (12)$$

at the free surface. (7)-(12) represent the set of equations to track the unsteady motion of the interface. The reader should note that these equations are in the contact line frame of reference and as such the flow rate is not Q' but $Q' - V_{cl}h$. Careful inspection of (7)-(12) indicates that 2 boundary conditions on y_1 and p are needed. The equations are elliptic in nature and hence the boundary conditions need to be specified on each end of the boundary i.e. at $x = 0, \infty$. These are $y_1(0,t) = 0$ (since the problem is analyzed in a contact line moving frame of reference) and $y_{1x}(\infty,t) = 0$ on y_1 and $p(\infty,t) = 0$ and a suitable flow rate matching condition on $p_x(0,t)$ which will be described in detail later. The initial interface shape $y_1(x,0)$ is prescribed to start the numerical integration with.

5 The pressure boundary condition at the liquid-gas interface

The correct boundary condition on p_x must be derived from the matching condition. The most commonly and widely accepted boundary condition used is the Reynolds condition (p = 0 and p_n = 0) at the liquid-gas interface, first proposed by Reynolds (1886) in his original paper on hydrodynamic lubrication. In the present case, the p_n = 0 (Neumann) boundary condition needs to be modified so the interface shape can be computed. And, we must include a boundary condition that incorporates the contact line condition discussed above.

To do this, the non-homogeneous boundary condition for p_n is derived at the contact line based on the momentum equation and continuity. Referring to Figure 6, the pressure gradient in Region 1 is set by the flow rate and is a constant for a given geometry. Conserving x-momentum equation in Region 1, subject to the no slip boundary conditions on two walls, we can derive the velocity profile. The flow rate is given by integration,

$$Q' = \frac{Uh}{2} - \frac{h^3 p_x(x<0)}{12\mu}. \quad (13)$$

In Region, 2 the governing equation for momentum is still the same but the boundary condition on the interface is zero shear stress condition that causes a velocity discontinuity at $x = 0$. The origin has a stress singularity that is well documented, especially if the contact line is moving. We only crudely model that here by matching fluxes across the $x = 0$ plane. Integrating this profile,

we get for region 2

$$Q = \frac{p_x(x>0)}{\mu}\big(\frac{y_1^3 - h^3}{3} + y_1 h(h-y_1)\big) + U(h-y_1) - V_{cl}h \quad (14)$$

Q is the flow rate at any x location and is a constant for a steady interface. In the unsteady case, it is a function of x.

The only location in Region 2 where we can match the flow rates at all times is at $x = 0$ in a frame of reference moving with the contact line. Thus,

$$\frac{Uh}{2} - \frac{h^3 p_x(x<0)}{12\mu} - V_{cl}h = \frac{p_x(x>0)}{\mu}(\frac{-h^3}{3}) + Uh - V_{cl}h, \quad (15)$$

$$4p_x(x>0) - p_x(x<0) = 6. \quad (16)$$

since $y_1 = 0$ at the matching location. In (16), p_x is nondimensionalized with $\mu U/h^2$. Thus, the right boundary condition to be prescribed that satisfies continuity and at the same time allows for a nontrivial interface shape is

$$p_x = 3\big(1 - \frac{Q'}{Uh}\big). \quad (17)$$

This is obtained on equating the incoming flow rate $Q' - V_{cl}h$ with the right hand side of (16) evaluated at the contact line. This universal boundary condition should be used instead of the standard Reynolds boundary condition at the contact line location. The condition is truly independent of the velocity of contact line or the dynamic contact angle and depends only on the nondimensional flow-rate Q'/Uh. If Q'/Uh is greater than 1, then p_x is negative and both the Couette and Poiseuille action are assisting the oil and aeration is highly unlikely to occur. When Q'/Uh is less than 1, Poiseuille and Couette actions are in opposite directions and this would promote aeration.

6 An axisymmetric model of a two-dimensional flow

The formulation mentioned in section 4 can be modified to incorporate the effect of constant body forces. This works well for cylindrical geometries provided $R_o - R_i \ll R_m$. A shortcoming of modeling a cylindrical geometry in this manner is that the influence of nonconstant body force cannot be incorporated. In the case of clutches, the change in the body force as the contact line moves from one radial location to another causes the contact line to stop. This effect cannot be included in the model of section 4. The model mentioned in this section is derived using the same underlying principles as explained above but employs cylindrical coordinates.

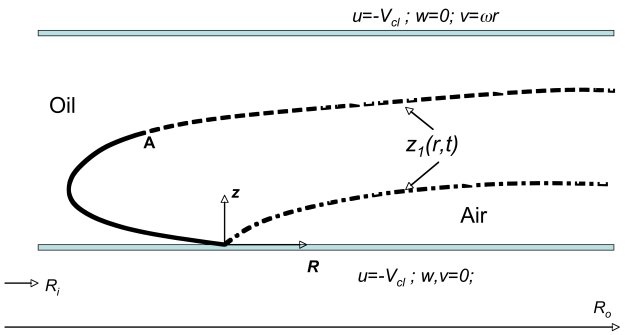

Figure 7: The geometry of the axisymmetric, two-dimensional model. The two interfaces shown are for the two ranges of contact angle, θ_c, given by a solid line ($0^o < \theta_c < 90^o$) and by the dash-dot line ($90^o < \theta_c < 180^o$). The dashed line indicates the region where the lubrication equations are solved. The solid line is the portion of the interface that is modeled by a third order polynomial. Three matching conditions link the two regions at junction point A where R = -r_o.

Let us consider an axisymmetric geometry when $90^o < \theta < 180^o$. The sketch and velocity components are shown in fig 7. A local coordinate system with orthogonal basis R, z and θ is placed on and moved with the contact line while the global system is fixed and has the basis r, z and θ. The reduced momentum equations are

$$-\frac{\rho v^2}{r} = -p_r + \mu u_{zz}, \quad (18)$$

$$-p_z = 0, \quad (19)$$

$$v_{zz} = 0. \quad (20)$$

where subscripts denote differentiation. The u and v components of velocity are obtained by integrating the above equations. The w component of velocity is obtained from the continuity equation in radial coordinates

$$w_z + \frac{1}{r}(ur)_r = 0. \quad (21)$$

The u, v, w components evaluated in the two-phase region with the interface shape defined as $z_1(r,t)$ are,

$$u = \frac{p_r}{2\mu}(z^2 - 2z_1(z-h) - h^2) - \frac{\rho\omega^2 r}{12\mu h^2}(z^4 - 4z_1^3(z-h) - h^4) - V_{cl}, \quad (22)$$

$$w = \frac{p_r}{2\mu} z_{1r}(z-h)^2 - \frac{1}{\mu}(\frac{p_r}{r} + p_{rr})(\frac{z^3}{6} - \frac{h^2 z}{2} - z_1(\frac{z^2}{2} - hz) + \frac{h^3}{3} - \frac{z_1 h^2}{2}) - \frac{\rho\omega^2 r}{2\mu h^2} z_1^2 z_{1r}(z-h)^2 + \frac{2\rho\omega^2}{\mu h^2}(\frac{z^5}{60} - \frac{h^4 z}{12} - \frac{z_1^3}{3}(\frac{z^2}{2} - hz) + \frac{h^5}{15} - \frac{z_1^3 h^2}{6}) + \frac{V_{cl}}{r}(z-h), \quad (23)$$

$$v = \omega r z/h. \quad (24)$$

The model requires one initial condition and two conditions on pressure and the interface, z_1, at $R = 0$ and ∞. The boundary condition on pressure at the contact line is derived in a similar manner, as the Cartesian model, based on continuity and momentum equation. However, as the contact line moves to a different radial location, this boundary condition changes. This dependence of $p_r(R = 0)$ on the value of radius r captures the effect of the non constant body force and the contact line stopping at a different radius for same flow rate and rotation speed.

$$p_r(R = 0) = (Q' - \frac{\rho\omega^2 r h^3}{15\mu})(-3\frac{\mu}{h^3}). \quad (25)$$

Knowing u, v and w and the boundary conditions on z_1 and p at $R = 0, \infty$ we advance interface shape using the kinematic boundary condition.

In the case where $0^o < \theta < 90^o$ and the oil wets the plate, the above analysis needs to be modified. For one, the shape of the interface is shown in figure 7 and is multivalued in z for a given radius. Secondly, the high slope near the nose of the interface inhibits the use of lubrication theory throughout. The lubrication theory can be applied in the upper and lower branches of the interface and the nose approximated as a spherical cap or some other polynomial that is atleast C^1 continuous, that is, the z location and the slope at the z location match. But the velocities in the lower branch are very small, so we choose to approximate the entire nose and the lower branch using a suitable ordered polynomial.

The first point in the upper branch (point A) where the lubrication equations are solved communicates with the third order polynomial. The slope and the z location of this point are used as two junction conditions. The third condition is the 'pinned' condition at the contact line. The fourth condition is based on p_r and the incoming flow rate similar to section 5. These four conditions define a third-order polynomial. Let us define the problem and the solution method.

The location of the interface at any time is $z_1(r, t)$. r_o is the R location of the point A in the upper branch where the lubrication equations are solved from. To ensure that the lubrication approximations are valid at all points lying at $R > r_o$, r_o is defined as a point where the slope of z_1 is at a predetermined value. This value is arbitrarily chosen to be between 0.9 and 1.4. We will discuss about the sensitivity of this value on the final solution below. During the calculation, the computational points are moved so that r_o remains at the location where the slope is at the predetermined value and the lubrication equations are valid.

The slope $z_{1r}(r_o, t)$ and location $z_1(r_o, t)$ are the two junction conditions prescribed to define the polynomial. The pinned condition at the contact line is the third condition. The fourth condition required is obtained from the flow rate such that

$$Q = \int_{z_1(r_o)}^{h} u dz. \quad (26)$$

where u, v and w are given by (22-24). The polynomial is thus modified at the end of each time step depending on the slope and z location at r_o.

The selection of a third-order polynomial based on the junction conditions ensures that the initial condition is very smooth. Kinematic boundary condition is used to advance the shape of the interface but a minor modification is now needed since we cannot take partial derivatives with respect to time if r is not constant due to sliding. Thus the kinematic boundary condition is

$$\frac{dz_1}{dt} + (u - u_{node})\frac{\partial z_1}{\partial r} = w, \quad (27)$$

where u_{node} is the velocity of sliding nodes in the upper branch to accommodate changing slope. The methodology for modeling the axisymmetric 'wetting' case involves a region where the lubrication equations are solved for ($r > r_o$) and a third order polynomial approximating the nose and the lower branch. Explicit solutions of these non-linear equations are unstable. Hence, we employ a predictor corrector scheme, where for each time step, the first iteration is done explicitly followed by three corrector iterations. The measured contact angles were used in the model, and the comparison between the theory and experimental inception conditions is good. The comparisons of this model's results with the clutch experiment are shown in Figure 8. The data in the single-phase region is obtained from Aphale et al. (2006).

To ensure robustness of the model, we performed a few tests. The model was run for two different values of slopes 0.9 and 1.2 to check the sensitivity on the predicted onset of aeration. The dependence of changing the slope was negligible. Second, we determined that it was acceptable to use a polynomial in the lower branch in the vicinity of the contact line instead of resolving this region using the lubrication equations. The curvature of the polynomial, as it changes its shape is compared with

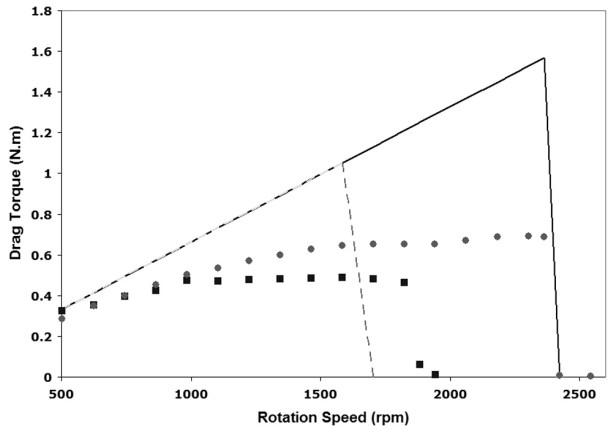

Figure 8: The drag torque, T, versus the rotation rate, ω, as computed with the axisymmetric, two-dimensional lubrication model, illustrating the influence of the contact angle on the inception of aeration. The experimental data for the aluminum plate $\theta_c = 9^o$ (o) and the Teflon coated plate with $\theta_c = 45^o$ (square) are shown with the analytical results with $\theta_c = 9^o$ (solid line) and $\theta_c = 45^o$ (dashed line). A larger contact angle, θ_c, indicates a lesser affinity for the liquid, and, as a result, aeration is promoted as the contact angle increases.

the curvature given in this region using the standard lubrication equation, and they are equivalent. Finally, the aeration onset differs depending on the initial location of the interface, whether it is at the inner radius or outer radius owing to the difference in the body force. This 'hysteresis' region in the model is 100-150 rpm and on the same order as observed in the experiments.

7 Conclusions

The effect of surface tension and contact angle on the onset of aeration in lubricating flows is significant. Hence, lubrication models that include aeration must consider the contact line conditions. The simple model presented in this work is an extension of that presented by Bretherton for aerating lubrication flow in axisymetric coordinates. The model includes the dynamics of the contact line, and it was shown to capture the basic elements of the aerating flow between a rotating and stationary disk with varying contact angle. The modified Bretherton's analysis can be used $a\ posteriori$ to predict the shape of the interface if a steady state solution exists, while the Reynolds boundary condition of $p_n = 0$ yields a trivial solution for the shape of the interface for two-dimensional flow. Thus, the standard Reynolds boundary condition needs to be modified. We propose a simple boundary condition as an alternative based on continuity and momentum equation. The boundary condition depends on the non-dimensional flow rate. The shape of the interface must be tracked and include the underlying shape and curvature of the interface near the contact line. And, this model was successfully used to predict the onset of aeration for the oil flow between two rotating disks with varying levels of oleophobicity.

References

APHALE, C, CHO, J, SCHULTZ, W, CECCIO, S, YOSHIOKA, T & HIRAKI, H 2006 Modeling and Parametric Study of Torque in Open Clutch Plates. *J. Tribology* **128**(2), 422–430.

APHALE, C, SCHULTZ, W & CECCIO, S 2010 The influence of grooves on the fully-wetted and aerated flow between open clutch plates. *J. Tribology* **132**(1).

BRETHERTON, F 1961 The motion of long bubbles in tubes. *J. Fluid Mech.* **10**, 166–188.

DUSSAN, E 1979 On the spreading of liquids on solid surfaces:static and dynamic contact lines. *Ann. Rev. Fluid Mech.* **11**, 371–400.

FISH, R 1991 Using the SAE No.2 Machine to Evaluate Wet Clutch Drag Losses. *SAE Technical Paper Series No. 910803* .

HOCKING, L 1976 A moving fluid interface on a rough surface. *J. Fluid Mech.* **76**, 801–817.

LLOYD, F 1974 Parameters Contributing to Power Loss in Disengaged Wet Clutch Drag Losses. *SAE Paper No. 740676* .

REYNOLDS, O 1886 On the theory of lubrictaion and its application to Mr. Beauchamp Tower's experiments, including an experimental determination of the viscosity of olive oil. *Philos. Trans. R. Soc. London* **177**, 157–234.

SCHADE, C 1971 Effects of Transmission Fluid on Clutch Performance. *SAE Paper No. 710734* .